ISSN 1330–0016
CODEN FIZBE7

TARGET FRAGMENTATION IN ^{28}Si-AgBr INTERACTIONS AT 14.5 AGeV – EVIDENCE FOR TWO- AND MANY-PARTICLE DYNAMICAL CORRELATIONS

D. GHOSH, A. DEB, S. BHATTACHARYYA, M. MONDOL, R. DAS, J. GHOSH, K. CHATTOPADHAYAY, R. SARKAR, S. MUKHERJEE, S. BISWAS, P MONDAL, K. Kr. PATRA, I. DUTTA, S. R. SAHOO, P. HALDAR, S. PRASAD and S. GHOSH

Nuclear and Particle Physics Research Centre, Department of Physics, Jadavpur University, Kolkota 700–032, INDIA

Received 24 July 2001; revised manuscript received 30 July 2002
Accepted 6 September 2002 Online 7 February 2003

This paper reports an investigation of the two-particle and three-particle short-range angular correlations among the target fragments produced in ^{28}Si–AgBr interactions at 14.5 AGeV. The experimental data have been compared with Monte Carlo simulated events to extract dynamical correlations. The data exhibit strong two-particle and three-particle correlations among the target fragments. The data further indicate the occurrence of the so-called side splash phenomena and disfavour the evaporation model.

PACS numbers: 25.75-q, 25.70.Mn UDC 539.126

Keywords: relativistic heavy-ion interaction, target fragmentation, correlations

1. *Introduction*

In order to get an idea about the ultimate structure of matter, various observables were measured in the field of strong interactions of elementary particles at high and ultra-high energies during the last few decades. Experiments were performed with lepton–lepton, hadron–hadron, hadron–nucleus and nucleus–nucleus interactions at relativistic and ultra-relativistic energies in order to reveal the underlying dynamics of multi-particle production process.

In previous investigations, emphasis was given mainly on pions [1] because pions are most frequently produced particles in high-energy collisions and the knowledge of pion-production mechanism is essential for the understanding of main features of high-energy collisions. Very little attention was paid to the target-evaporated slow particles. But the target fragments, known as black particles in emulsion terminology, are not just spectators. They are emitted at the late stage of nuclear reactions and are expected to remember the parts of the history of interactions. So the appearance of the black particles is of great importance and it is a potential source of information. This less explored area should be probed with all available tools.

One of the well-known models of target fragmentation is the evaporation model [2]. According to this model, "shower" and "grey" tracks are emitted from the nucleus very soon after the instant of impact. This leaves the nucleus in a highly excited state. Indeed, the excitation energy may sometimes be comparable with the total binding energy of the nucleus. Emission of heavily charged particles from this state, however, now takes place relatively slowly. In order to escape from the residual nucleus, a particle must await a favourable statistical fluctuation arising out of random collisions among the nucleons. Emission occurs if, due to a fluctuation, the particle is both close to the nuclear boundary, travelling in an outward direction, and if its kinetic energy is greater than its binding energy. After the evaporation of this particle, a further relatively long period on a nuclear time scale, say 10^{-17} s, will commonly elapse before a second particle is also placed in conditions favourable for escape, and so on. The process continues until the excitation energy of the residual nucleus is so small that transition to the ground state is likely to be effected by the emission of gamma rays. In this model, in the rest system of the nucleus, the direction of emission of the evaporation particles is distributed isotropically. The evaporation model is based on the assumption that statistical equilibrium has been established in the decaying system and the lifetime is much longer than the time taken to distribute the energy among nucleons within the nucleus. In a very recent study [3], it has been shown that the angular distribution of target fragments from relativistic heavy-ion interactions could not be explained satisfactorily by the evaporation model.

One of the most interesting questions in this field is "What is the nature of the correlation among the target fragments?" It is possible to determine a correlation function (R) by which we can investigate the nature of the correlation among the target fragments. The correlation can give direct information about the late stage of the reaction when nuclear matter is highly excited and diffused [4]. Several studies using well-known two- and three-particle short-range correlation function have been reported in different types of interactions [5–19]. A few works have been performed where it was observed that target fragments seem to be emitted preferentially in a correlated fashion (see, e.g., Ref. [20]). However, it is not possible to say with certainty why this happens. One possibility are the so-called side splash phenomena. Stocker [21] first reported experimental evidence of side splash phenomena. According to him, when two nuclei collide centrally, a head shock zone is developed during the diving phase of the projectile nucleus within the target. A strongly compressed and highly excited projectile-like object continues to interpenetrate the target with supersonic velocity and pushes the matter sideward to form the shock wave, giving rise to the correlation in the sideward directions.

For a better understanding of the origin of the correlations, it is necessary to investigate data measured with different projectiles, covering the whole available energy spectrum. However, in the case of target fragments in nucleus–nucleus interactions at ultra-relativistic energies, such studies are rare. In this paper, we made an exhaustive investigation of two-particle and three-particle correlations in the emission angle space in the ^{28}Si–AgBr interaction at 14.5 AGeV.

2. Experimental details

The data were obtained from Ilford G5 emulsion stacks exposed to the 14.5 AGeV ^{28}Si beam from the Alternating Gradient Synchrotron (AGS) at Brookhaven National Laboratory (BNL) [22]. A Leitz Metaloplan microscope with a 10× objective and a 10× ocular lens, provided with a semi-automatic scanning stage, was used to scan the plates. Each plate was scanned by two independent observers to increase the scanning efficiency. The final measurements were performed using an oil-immersion 100× objective. The measuring system fitted with it has an 1 μm resolution along the X and Y axes and 0.5 μm resolution along the Z axis.

After scanning, the events were chosen according to the following criteria:

i) The incident beam track should not exceed more than 3° from the main beam direction in the pellicle. It is done to ensure that we have taken events due to the real projectile beam.

ii) Events showing interaction within 20 μm from the top and bottom surface of the pellicle were rejected. This was done to reduce the loss of tracks as well as to reduce the error in the angle measurements.

iii) The tracks of the incident particle, which induce interactions, were followed in the backward direction to ensure that they are due to the projectile beam starting from the beginning of the pellicle.

According to the emulsion terminology [2], the particles emitted after interactions are classified as:

A. Black particles: they consist of both single and multiple charged fragments. They are target fragments like carbon, lithium, berilium, etc., ions with ionization density higher than or equal to $10I_0$, where I_0 is the minimum ionization of singly-charged particles.

B. Grey particles: they are mainly fast target recoil protons with an energy up to 400 MeV. Their ionization is $1.4I_0 \leq I < 10I_0$. Their ranges are larger than 3mm and have velocities $0.7c \geq v \geq 0.3c$.

C. Shower particles: the relativistic shower tracks with ionization less then or equal to $1.4I_0$ are produced mostly by pions and are not generally confined within the emulsion pellicle. These shower particles have energy in the GeV range.

D. The projectile fragments are a different class or tracks with constant ionization, long range and small emission angle.

To ensure that the targets in the emulsion are silver or bromine nuclei, we choose only the events with at least eight heavy ionizing tracks of (black + grey) particles. The events which have the number of heavy tracks less than eight is due to the collision of the projectile beam with carbon, nitrogen and oxygen nucleus present in the emulsion. These types of events are called CNO events.

According to the above selection procedure, we have chosen 350 events of ^{28}Si–AgBr interactions at 14.5 AGeV. The average multiplicity of the events analyzed is 10.78. The emission angle (θ) and azimuthal angle (ϕ) are determined for each track by taking readings of the coordinates of the interaction point (X_0, Y_0, Z_0), the coordinates (X_1, Y_1, Z_1) at the end of the linear portion of each secondary track and the coordinates (X_i, Y_i, Z_i) of a point on the incident beam.

The uncertainty in the angle measurements is estimated to be of the order of a milliradian. Such a high resolution makes emulsion plate very effective for studying correlation phenomena.

3. *Method of analysis*

3.1. *Two-particle correlation*

For the phase-space variable z, the two-particle normalized correlation function is defined as

$$R(z_1, z_2) = \frac{\rho_2(z_1, z_2) - \rho_1(z_1)\rho_1(z_2)}{\rho_1(z_1)\rho_1(z_2)} = \frac{\rho_2(z_1, z_2)}{\rho_1(z_1)\rho_1(z_2)} - 1\,,$$

where the quantities $\rho_1(z) = (1/\sigma)(\mathrm{d}\sigma/\mathrm{d}z)$ and $\rho_2(z_1, z_2) = (1/\sigma)(\mathrm{d}^2\sigma/\mathrm{d}z_1\mathrm{d}z_2)$ represent one- and two-particle densities, respectively. R can be represent as

$$R = N_T \frac{N_2(z_1, z_2)}{N_1(z_1)N_1(z_2)} - 1\,,$$

where N_T is the total number of inelastic events. $N_1(z_1)$ is the number of black tracks in the phase space interval z_2, to $z_2 + \mathrm{d}z_2$, and $N_2(z_1, z_2)$ is the number of pairs of particles having one particle in the phase space interval z_1 to $z_1 + \mathrm{d}z_1$ and the other particle in z_2 to $z_2 + \mathrm{d}z_2$ of an event.

For the present work R in terms of $\cos\theta$ is represented as

$$R(\cos\theta_1, \cos\theta_2) = N_T \frac{N_2(\cos\theta_1, \cos\theta_2)}{N_1(\cos\theta_1)N_1(\cos\theta_2)} - 1\,. \qquad (1)$$

The idea of using the correlation function of the above form is attributed to Kirkwood [23] in statistical physics. $R = 0$ implies the absence of correlation, i.e. the case of completely independent particle emission.

3.2. Three-particle correlation

The three particle inclusive correlation function for phase space variable z can be defined as in Ref. [24],

$$R(z_1, z_2, z_3) = \frac{\rho_3(z_1, z_2, z_3) + 2\rho_1(z_1)\rho_1(z_2)\rho_1(z_3)}{\rho_1(z_1)\rho_1(z_2)\rho_1(z_3)}$$

$$- \frac{\rho_2(z_1, z_2)\rho_1(z_3) + \rho_2(z_2, z_3)\rho_1(z_1) + \rho_2(z_3, z_1)\rho_1(z_2)}{\rho_1(z_1)\rho_1(z_2)\rho_1(z_3)},$$

where the quantity

$$\rho_3(z_1, z_2, z_3) = \frac{1}{\sigma}\frac{\mathrm{d}^3\sigma}{\mathrm{d}z_1\mathrm{d}z_2\mathrm{d}z_3}$$

represents the three-particle density. ρ_1 and ρ_2 represent the same quantities as before in the case of the two-particle correlation.

In terms of the number of particles, R can be represented as

$$R(z_1, z_2, z_3) = N_T^2 \frac{N_3(z_1, z_2, z_3)}{N_1(z_1)N_1(z_2)N_1(z_3)} + 2$$

$$-N_T \frac{N_2(z_1, z_2)}{N_1(z_1)N_1(z_2)} - N_T \frac{N_2(z_2, z_3)}{N_1(z_2)N_1(z_3)} - N_T \frac{N_2(z_3, z_1)}{N_1(z_3)N_1(z_1)},$$

where $N_3(z_1, z_2, z_3)$ is the number of triplets of particles having one particle in the interval z_1 to $z_1 + \mathrm{d}z_1$, the other particle between z_2 to $z_2 + \mathrm{d}z_2$ and the third particle between z_3 to $z_3 + \mathrm{d}z_3$ in an event.

For our case,

$$R(\cos\theta_1, \cos\theta_2, \cos\theta_3) = N_T^2 \frac{N_3(\cos\theta_1, \cos\theta_2, \cos\theta_3)}{N_1(\cos\theta_1)N_1(\cos\theta_2)N_1(\cos\theta_3)} + 2 \qquad (2)$$

$$-N_T \frac{N_2(\cos\theta_1, \cos\theta_2)}{N_1(\cos\theta_1)N_1(\cos\theta_2)} - N_T \frac{N_2(\cos\theta_2, \cos\theta_3)}{N_1(\cos\theta_2)N_1(\cos\theta_3)} - N_T \frac{N_2(\cos\theta_3, \cos\theta_1)}{N_1(\cos\theta_3)N_1(\cos\theta_1)}.$$

4. Monte Carlo simulation

Apart from the presence of true dynamics, correlation among the target fragments may arise due to following reasons:

I) Board multiplicity distribution.

II) The dependence of the single-particle spectrum $(1/\sigma)(\mathrm{d}\sigma/\mathrm{d}z)$ on the multiplicity.

III) Trivial statistical fluctuations.

To search for the non-trivial dynamical correlation among the slow particles associated to the target, the experimental data have to be compared with those calculated using the Monte Carlo simulation.

We have utilized the framework of an independent emission hypothesis for simulation using the following assumptions:

i) The target fragments are emitted independently.

ii) The multiplicity distribution of the Monte Carlo events is the same as the empirical multiplicity spectrum of the real ensemble.

iii) The single-particle spectrum $(1/\sigma)(\mathrm{d}\sigma/\mathrm{d}z)$ of the simulated events reproduces the distribution $(1/\sigma)(\mathrm{d}\sigma/\mathrm{d}z)$ of the experimental data.

The difference between the experimental values and the Monte Carlo values can be interpreted as the dynamical surplus which arises due to some dynamics in the reaction process. The dynamical surplus can be written as

$$R_D = R - R_M \,, \tag{3}$$

where R is the experimental values R_M is the value obtained using the Monte Carlo simulation.

5. Results and discussion

5.1. Two-particle correlation

The two-particle normalized correlation function R has been calculated with the help of relation (1). Figure 1 shows the plot of the two-particle normalized correlation function R against $\cos\theta$ for the values of the diagonal elements $(\cos\theta_1 = \cos\theta_2 = \cos\theta)$ of the correlation matrices, characterizing the magnitude of the short-range correlation at different phase space intervals. The dots in the figure represent the experimental values and the full curve represents the values of the

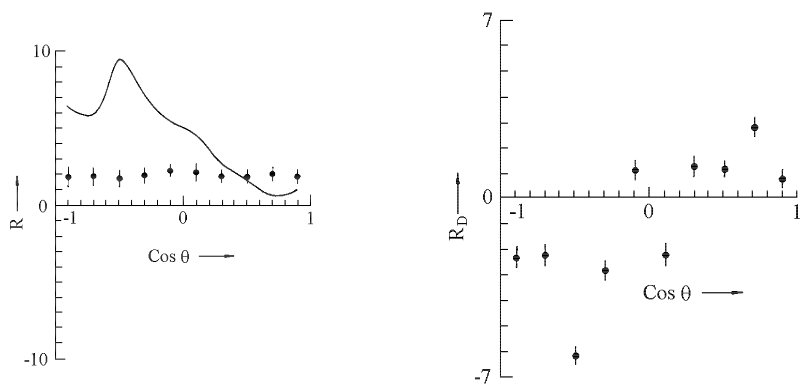

Fig. 1. Correlation function R against $\cos\theta$ in the case of two-particle correlation.
Fig. 2 (right). Dynamical surplus value R_D against $\cos\theta$ in the case of two-particle correlation.

correlation function calculated by the Monte Carlo simulation. The Monte Carlo events were generated following the assumption made in the previous section.

Figure 2 represents the dynamical surplus R_D due to two-particle correlations. It is evident from Fig. 2 that the dynamical surplus values are non–zero for any value of $\cos\theta$ which implies that the short-range two-particle dynamical correlation exists over the entire space of emission angle. From the graph it is further seen that the correlation is prominent at $\cos\theta$ values (-0.4 to -0.9) and 0.7 i.e. for emission angles around 113° to 154° and also near 45°.

5.2. Three-particle correlation

The three-particle normalized correlation function has been calculated for different values of $\cos\theta$ with the help of relation (2). The short-range correlation has been investigated by plotting the values of the diagonal elements of the correlation matrices ($\cos\theta_1 = \cos\theta_2 = \cos\theta_3 = \cos\theta$) against the $\cos\theta$ variable. The full curve in the Fig. 3 represents the values of the correlation function calculated by the Monte Carlo simulation and the dots represent the experimental values.

Figure 4 represents the dynamical surplus values R_D for the three-particle correlation. The figure shows that the short-range three-particle dynamical correlation exists over the entire $\cos\theta$ space. The three-particle correlation appears to be prominent at the emission angle $\cos\theta$ (-0.5 to -0.9) and (0.3 to 0.9), i.e. from emission angle 120° to 154° and also from 72° to 25°.

Angular distribution of the experimental and simulated data for the multiplicity bins $1-11$ are shown in Figs. 5a and 5b, respectively. Figures 5c and 5d represent the same results for the bins $12-22$. From the curves, it is seen that both the multiplicity bins distribution obtained from the simulated data and experimental data are similar in nature.

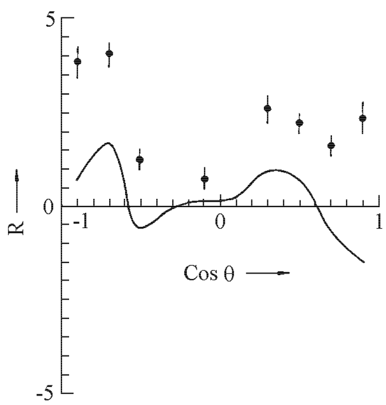

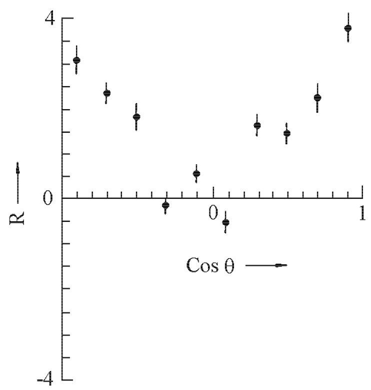

Fig. 3. Correlation function R against $\cos\theta$ in the case of three-particle correlation.
Fig. 4 (right). Dynamical surplus value R_D against $\cos\theta$ in the case of three-particle correlation.

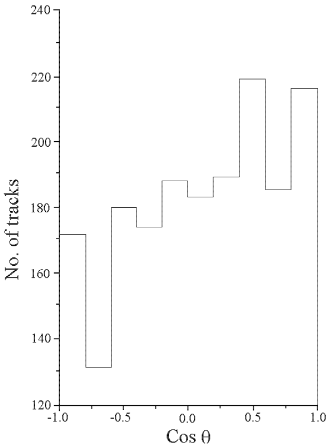

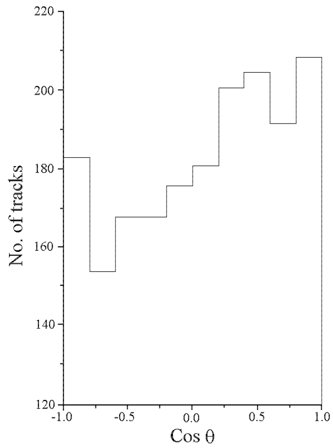

Fig. 5a. Angular distribution of $\cos\theta$ *in the multiplicity bin* $1-11$ *of experimental data.*

Fig. 5b (right). Angular distribution of $\cos\theta$ *in the multiplicity bin* $1-11$ *of simulated data.*

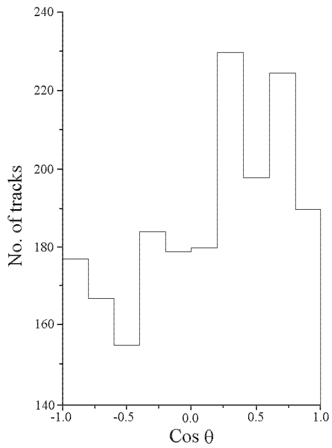

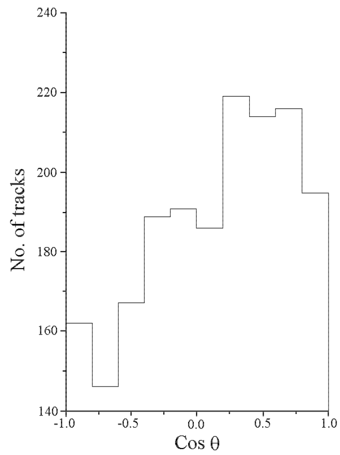

Fig. 5c. Angular distribution of $\cos\theta$ *in the multiplicity bin* $12-22$ *of experimental data.*

Fig. 5d (right). Angular distribution of $\cos\theta$ *in the multiplicity bin* $12-22$ *of simulated data.*

It is interesting to note that both two-particle and three-particle correlations exist in the backward and forward hemisphere. The angular zone of the correlation in the backward hemisphere may indicate the occurrence of the so-called side splash phenomena. However, the evidence of two- and many-particle dynamical correlations among target fragments speaks against the evaporation model. Thus, this analysis provides new data on two-particle and three-particle correlations in the $\cos\theta$ space which is not only interesting but also extremely useful for the understanding the emission of target fragments in high energy nucleus-nucleus interactions.

Acknowledgements

The authors are grateful to Prof. P. L. Jain, State University of Buffalo, Buffalo, U.S.A. for providing them with the exposed and developed emulsion plates used for this analysis. We also like to acknowledge the financial help by the University Grant Commission (Govt. of India) under their COSIST programme.

References

[1] E. L. Berger, Nucl. Phys. B **85** (1975) 61; A. M. Chao and C. Quigg, Phys. Rev. D **9** (1974) 2016; C. Quigg, p. Pirilla and G. H. Thomas, Phys. Rev. Lett. **34** (1975) 2091.

[2] C. F. Powell, P. H. Fowler and D. H. Perkins, *The study of elementary particles by photographic method*, Oxford, Pergamon, p. 450–464 and references therein.

[3] D. Ghosh, A. Ghosh, P. Ghosh and D. Kundu, J. Phys. G: Nucl. Phys **20** (1994) 1077.

[4] G. Giacomelli and M. Jacob, Phys. Rep. **55** (1979) 1.

[5] J. Plutta et al., Euro. Phys. Jour. A **9** (2000) 63.

[6] A. B. Larionov, Euro. Phys. Jour. A **7** (2000) 507.

[7] D. V. Anchishkin, Euro. Phys. Jour. A **7** (2000) 229.

[8] A. El. Naghy et al., Nuovo Cimento A **110** (1997) 125.

[9] A. Breakstone et al., Mod. Phys. Lett. A **6** (1991) 2785.

[10] D. Ghosh et al., Phys. Rev. D **26** (1982) 2983.

[11] D. Ghosh et al., Acta Phys. Slov. **47** (1997) 425.

[12] I. Derado, G. Jancso and N. Schmitz (EMC), Z. Phys. C **56** (1992) 553.

[13] G. Singh and P. L. Jain, J. of Phys. G **23** (1997) 1655.

[14] P. L. Jain and G. Singh, Nucl. Phys. A **596** (1996) 700.

[15] N. Suzuki and M. Biyajima, Phys. Rev. C **60** (1999) 034903.

[16] G. Alexander and E. K. G. Sarkisyan, Nucl. Phys. B **92** (2001) 211.

[17] G. Alexander and E. K. G. Sarkisyan, Phys. Lett. B **487** (2000) 215.

[18] N. N. Abd Allah, Int. J. Mod. Phys. E **10** (2001) 55.

[19] M. Goncalves et al., Euro. Phys. Jour. A **7** (2000) 435.

[20] D. Ghosh, K. Purkait and R. Sengupta, Acta Phys. Slov. **47** (1997) 425.

[21] H. Stocker, J. A. Maruhn and W. Greiner, Z. Phys. A **293** (1979) 173.

[22] P. L. Jain and G. Shing, Phys. Rev. C **44** (1991) 854.

[23] I. Kirkwood, J. Chem. Phys. **7** (1935) 919.

[24] E. M. Levin, M. G. Ryskin and N. N. Nikolaev, Z. Phys. C **5** (1980) 285.

Appendix: Calculation of Errors

Experimentally, the two-particle correlation function in the emission angle phase space is calculated as

$$R(\cos\theta_1, \cos\theta_2) = \frac{< n_1 n_2 >}{< n_1 >< n_2 >} - 1$$

for $\cos\theta_1 \neq \cos\theta_2$, and

$$R(\cos\theta_1, \cos\theta_2) = \frac{< n(n-1) >}{< n >^2} - 1$$

for $\cos\theta_1 = \cos\theta_2$, where n_1 and n_2 are the black multiplicities in a small interval of $\delta(\cos\theta)$ around $\cos\theta_1$ and $\cos\theta_2$. Thus the variance in R is calculated term by term, and instead of giving the long algebraic expression of the net variance, we have computed it and shown the corresponding errors in the figures.

The three-particle correlation function is experimentally obtained using the relation

$$R(\cos\theta_1, \cos\theta_2, \cos\theta_3) = \frac{< n(n-1)(n-2) >}{< n >^3} - \frac{3 < n(n-1) >}{< n >^2} + 2$$

for $\cos\theta_1 = \cos\theta_2 = \cos\theta_3$.

The variance of this quantity is calculated term by term, and instead of giving a long algebraic expression of net variance we have computed it and shown the corresponding errors in the figures.

RAZBIJANJE JEZGRI U SUDARIMA ^{28}Si-AgBr NA 14.5 AGeV – PODACI O DVO- I VIŠEČESTIČNIM DINAMIČKIM KORELACIJAMA

Izvješćujemo o istraživanju dvo- i tročestičnih kratko-dosežnih korelacija dijelova mete proizvedenih u sudarima ^{28}Si–AgBr na 14.5 AGeV. Eksperimetalni se podaci uspoređuju s oponašanima izračunatim Monte Carlo metodom radi razdvajanja dinamičkih korelacija. Podaci ukazuju na pojavu tzv. pljuštenja (engl. “splash”) i nisu u skladu s modelom isparavanja.